PHYSICAL REVIEW C **75**, 051304(R) (2007)

Decay of ^{10}C excited states above the $2p + 2\alpha$ threshold and the contribution from "democratic" two-proton emission

R. J. Charity,[1] K. Mercurio,[2] L. G. Sobotka,[1,2] J. M. Elson,[1] M. Famiano,[3] A. Banu,[4] C. Fu,[4] L. Trache,[4] and R. E. Tribble[4]
[1]*Department of Chemistry, Washington University, St. Louis, Missouri 63130, USA*
[2]*Department of Physics, Washington University, St. Louis, Missouri 63130, USA*
[3]*Department of Physics, Western Michigan University, Kalamazoo, Michigan 49008, USA*
[4]*Cyclotron Institute, Texas A&M University, College Station, Texas 77843, USA*
(Received 28 February 2007; published 31 May 2007)

The decay of ^{10}C excited states to the $2p + 2\alpha$ exit channel has been studied using an $E/A = 10.7$ MeV ^{10}C beam inelastically scattered from a ^{9}Be target. Levels associated with two-proton decay to the ground state of ^{8}Be have been observed. These include states at 5.18 and 6.54 MeV which decay by sequential two-proton emission through the long-lived ground state of ^{9}B. In addition, states at 5.3 and 6.57 MeV were found in which there is no long-lived intermediate state between the two proton emissions. For the 6.57 MeV state, the two protons are preferably emitted on the same side of the decaying ^{10}C fragment.

DOI: 10.1103/PhysRevC.75.051304 PACS number(s): 27.20.+n, 23.50.+z, 23.60.+e, 25.60.Gc

The level structure of ^{10}C is not well known. Figure 1 shows the low-lying levels that have been identified so far [1]. Only the first excited state (2^+, $E^* = 3.351$ MeV), which decays by γ-ray emission, is fully characterized and all other excited states are particle unstable. Common particle decay modes, such as proton or α-particle emission, produce daughter nuclei, ^{9}B and ^{6}Be, which are also particle unstable. Both of these nuclei decay, either directly, or via an intermediate step, and lead to the $2p + 2\alpha$ exit channel. The threshold for $^{10}\text{C} \rightarrow {}^{3}\text{He} + {}^{7}\text{Be}$ decay is 15.0 MeV. This is the first binary decay mode that leads to two particle-stable fragments. All excited states with excitation energies between this threshold and the $2p + 2\alpha$ threshold must decay in some manner to the $2p + 2\alpha$ exit channel. Figure 1 also shows possible intermediate states in neighboring nuclei and their decays which could contribute to the $2p + 2\alpha$ channel.

The structure of ^{10}C is expected to be similar to its mirror nucleus ^{10}Be. Both nuclei are predicted to have strong α-particle cluster structure [2]. Rotational bands based on the two molecular configurations each consisting of a two-alpha (^{8}Be) core and two valence neutrons [2] have been identified in ^{10}Be [3]. The 0^+ ground and 2^+ first excited state in ^{10}C are presumably members of one of these rotational bands. One would like to identify members of the higher-lying rotational band built on a second more deformed 0^+ level.

The excited states of ^{10}C may undergo two-proton decay. This could be a sequential two-proton emission passing through a long-lived intermediate as in the decay of the ground state of ^{12}O [4]. Alternatively, a more direct three-body breakup or democratic decay could occur as in the case of ^{6}Be [5,6].

Due to the potentially interesting features of ^{10}C levels, we have studied the decay of inelastically excited ^{10}C nuclei to the $2p + 2\alpha$ exit channel. Correlations between the four detected particles were analyzed and used to assign the decay paths of all observed levels. At the Texas A&M University cyclotron facility, a primary beam of $E/A = 15.0$ MeV ^{10}B of intensity 40 pnA was extracted from the K500 cyclotron. This beam impinged on a hydrogen gas cell held at a pressure of two atmospheres and kept at liquid-nitrogen temperature. A secondary beam of $E/A = 10.7$ MeV ^{10}C was produced through the $^{10}\text{B}(p,n)^{10}\text{C}$ reaction and separated from other reaction products using the MARS spectrometer [7]. This secondary beam, with intensity of 5×10^4 s^{-1}, purity of 99.5%, and an energy spread of 3%, impinged on a 14 mg/cm^2 target of ^{9}Be. The beam spot on the target was 3.5 mm $\times$ 5.3 mm in area.

Charged particles produced in the interactions were detected in four Si E-ΔE telescopes located in a plane 14 cm downstream of the target. The telescopes, part of the HIRA array [8], consisted of a 65 μm thick, single-sided Si-strip ΔE detector followed by a 1.5 mm thick, double-sided Si strip E detector. All Si detectors were 6.4 cm $\times$ 6.4 cm in area with the position-sensitive faces divided into 32 strips. The telescopes were positioned in a square arrangement with each telescope offset from its neighbor to produce a small, central, square hole through which the unscattered beam passed. With this arrangement, the angular range from $\theta = 1.3$ to 7.7° was covered. Signals produced in the telescopes were read out with the HINP16C chip-readout electronics [9].

Energy calibrations were obtained from the p, d, t, and α-particle "punch through" energies. Energy-loss corrections accounting for the traversal of the fragments through half of the target thickness were derived from Ref. [10].

In order to determine the efficiencies for detecting the $2p + 2\alpha$ events and the resolution of the reconstructed excitation energy, Monte Carlo simulations were performed. As a test of these simulations, we first looked at ^{12}C states which decay into the 3α channel. These events were formed in the $^{9}\text{Be}(^{10}\text{C},^{12}\text{C})^{7}\text{Be}$ and possibly other more complex reactions. In Fig. 2, the distribution of reconstructed ^{12}C excitation energy is plotted as the histogram for 3α events detected in this work. Two prominent peaks are observed associated with the known $E^* = 7.65$ MeV (0^+, $\Gamma = 8.5$ eV) and $E^* = 9.64$ MeV (3^-, $\Gamma = 34$ keV) states. The widths of the peaks are significantly larger than the intrinsic widths,

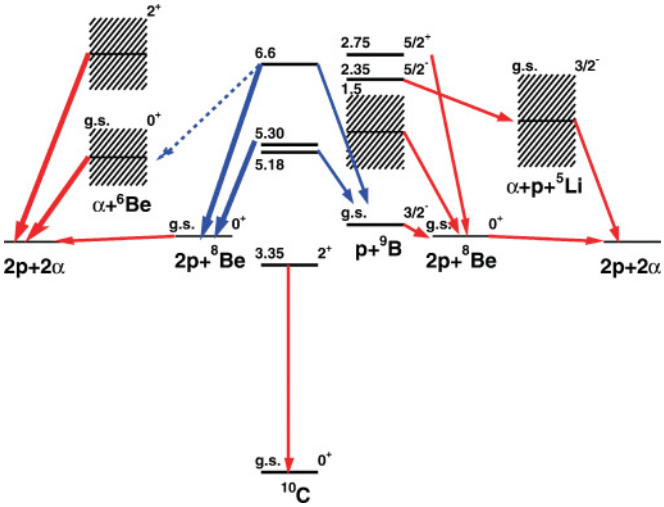

FIG. 1. (Color online) The level scheme of ^{10}C and other nuclei of interest in its particle decay. Arrows indicate known transitions and those established in this work. The thick arrows indicate democratic two-proton emission.

indicating the importance of the experimental resolution. In the Monte Carlo simulations, the decay of these states was treated as a sequential α particle emission through the unstable intermediate ^{8}Be$_{g.s.}$. In these, and subsequent simulations, the interaction depth in the target was chosen randomly, the effects of energy loss [10] and small-angle scattering [11] on the particles as they leave the target were included. The simulated events were passed through a detector filter and the energy and position resolution of the detectors were added. Subsequently, the events were analyzed in the same manner as the experimental events. For each state, the primary energy and angular distributions of the parent fragments were chosen such that the reconstructed distributions for the "detected" events in the simulations reproduced the equivalent experimental results. These simulations reproduce the experimental ^{12}C peak energies and widths quite well.

For each detected $2p + 2\alpha$ event, a ^{10}C excitation energy $E^*(^{10}\mathrm{C})$ was reconstructed from the kinetic energy released in the disassociation of the ^{10}C state minus the decay Q-value (-3.726 MeV). The former was determined as total kinetic energy of the four detected particles in their center-of-mass

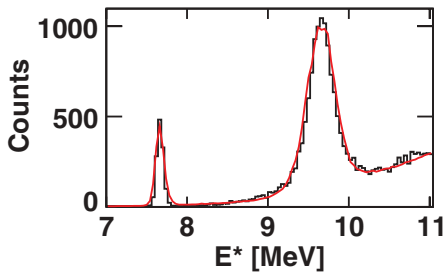

FIG. 2. (Color online) The ^{12}C excitation-energy distribution from 3α events. The histogram shows the experimental distribution, while the curve gives the predictions of the Monte Carlo simulations. An additional exponential background was added to the simulated results to aid in the comparison with the data.

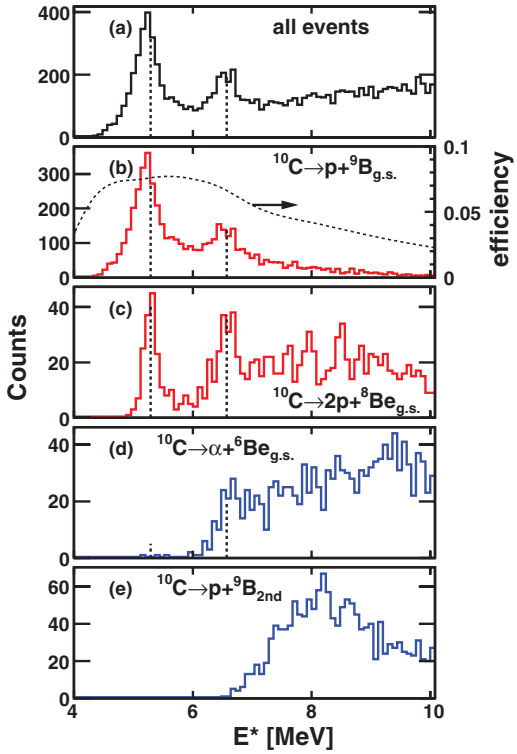

FIG. 3. (Color online) Experimental distribution of reconstructed excitation energy: (a) All detected $2p + 2\alpha$ events. (b)–(e) Event groups one to four. As reference, the vertical dashed lines indicate the centroids of the two prominent peaks in panel (c) associated with the second group. In (b), the simulated efficiency for detecting events initiated by a $p + {}^{9}\mathrm{B}_{g.s.}$ decay is indicated by the dashed curve.

frame. The distribution of $E^*(^{10}\mathrm{C})$ is shown in Fig. 3(a). This spectrum shows two broad peaks at $\sim$5.2 and $\sim$6.5 MeV, each with a FWHM of $\geqslant$350 keV. The experimental resolution determined from the simulations are 190 keV and 240 keV for the two peaks, respectively, indicating that both peaks have significant intrinsic width.

Many previous experimental studies have observed peaks close to these energies [12–16]. Benenson *et al.* [13] measured widths for both states of 300 ± 50 keV. Schneider *et al.* [17] fit a width of 190 ± 35 keV for the 6.5 MeV peak. The lower-energy peak was fit with an unresolved doublet with centroids of 5.22 ± 0.04 and 5.38 ± 0.07 MeV and widths of 225 ± 45 keV and 300 ± 60 keV, respectively. It is possible that one, or both, of the peaks observed in Fig. 3(a) are at least doublets. The 5.2 MeV region in ^{10}C is expected to have analogs in the 6 MeV region of the mirror nucleus ^{10}Be, where there is a quadruplet of states separated by 305 keV [1]. For the 6.6 MeV peak, the analogous region in ^{10}Be is 7.5 MeV where there is a doublet. If the individual states in these multiplets decay by different mechanisms, then it may be possible to separate them based on the correlations between the final particles.

For each $2p + 2\alpha$ event, we first looked for correlations between the two α particles associated with ^{8}Be decay. The reconstructed distribution of ^{8}Be excitation energy $E^*(^{8}\mathrm{Be})$ is plotted in Fig. 4(a). It displays a sharp peak at $E^*(^{8}\mathrm{Be}) = 0$ MeV corresponding to the decay of the ground state of

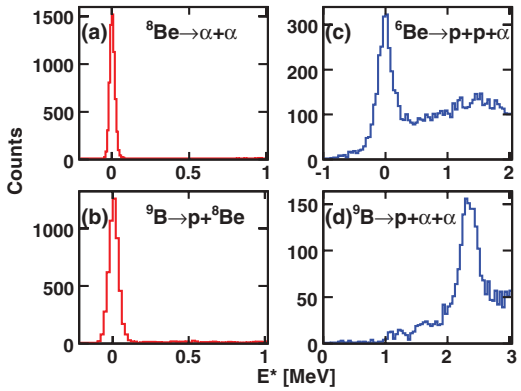

FIG. 4. (Color online) Experimental distributions of reconstructed excitation energy: (a) for ^{8}Be fragments from α-α pairs. (b) ^{9}B fragment from p + ^{8}Be$_{g.s.}$ correlations. (c) ^{6}Be fragments from $p + p + \alpha$ events. (d) ^{9}B fragments from $p + \alpha + \alpha$ events which do not decay through ^{8}Be$_{g.s.}$.

^{8}Be ($\Gamma = 7$eV). This peak has a FWHM of 35 keV, a value consistent with the simulated result.

For events with a ^{8}Be$_{g.s.}$ correlation, we then looked for $p + ^8$Be correlations associated with the decay of ^{9}B. For each $2p + 2\alpha$ event, there are two ways of choosing a $p + 2\alpha$ subset. A ^{9}B excitation energy is determined for each subset, but only the minimum value is kept. The distribution of $E^*(^9\mathrm{B})$ is plotted in Fig. 4(b). Again there is a sharp peak at $E^*(^9\mathrm{B}) = 0$ MeV corresponding to the decay of the ground state of ^{9}B ($\Gamma = 0.5$keV) with a FWHM of 85 keV, the latter is consistent with the simulated value.

For events without a ^{8}Be$_{g.s.}$ correlation, we have looked for $2p + \alpha$ correlations associated with ^{6}Be decay. Again there are two ways of choosing a $2p + \alpha$ subset, and the one with the minimum excitation energy was taken. The second excited state of ^{9}B ($E^* = 2.35$ MeV) alpha decays to a ^{5}Li intermediate and thus we have also looked for this correlation in $p + 2\alpha$ subsets. The distributions of $E^*(^6\mathrm{Be})$ and $E^*(^9\mathrm{B})$ from events without ^{8}Be$_{g.s.}$ correlations are plotted in Figs. 4(c) and 4(d), respectively. Peaks associated with ^{6}Be$_{g.s.}$ and ^{9}B$_{2nd}$ are well resolved.

From these correlations we have subdivided all $2p + 2\alpha$ events into four groups. The first group contains those events associated with $p + ^9$B$_{g.s.}$ decay. Their excitation energy distribution is plotted as the histogram in Fig. 3(b). The predicted efficiency for detecting these events is indicated by the dashed curve. A large fraction of the $2p + 2\alpha$ events with $E^*(^{10}\mathrm{C}) < 6$ MeV are in this group and the two peaks at ~5.2 and ~6.5 MeV are still clearly visible. The second group contains those events with a ^{8}Be$_{g.s.}$ correlation, but no ^{9}B$_{g.s.}$ correlation. There are fewer of these events compared to the first group, however their excitation energy distribution shown in Fig. 3(c) also shows two significant peaks. The mean peak energies and estimates of the intrinsic widths and cross sections determined from the simulated resolution and efficiency are listed in Table I. The higher-energy peaks, in both groups, have consistent centroids and widths. Therefore either these are two decay branches of a single state or a closely spaced doublet. On the other hand, the centroid and widths for the lower-energy peaks are not consistent (Table I). This is highlighted in Fig. 3(b), where the peak positions for the first group can be compared to the dashed lines giving the centroids from the second group. There is an offset of ~100 keV between the lower-energy peaks in the two groups. As the widths of these peaks are also not the same, these data support the claim of Schneider *et al.* [17], that there are two levels in this region. While it is possible for two different decay channels from the same level to exhibit different experimental energies and widths (due to calibration errors and efficiency effects) we think this unlikely in the present case, because the detected fragments are the same ($2p + 2\alpha$) with energies near that of the beam ($E/A \sim 10$ MeV).

TABLE I. Mean excitation energies, intrinsic widths, and cross sections associated with the peaks observed for each of the different event groups. The results are corrected for detector resolution and efficiency.

Group	Decay	$\langle E^* \rangle$ MeV	Γ keV	σ mb
1	$p + ^9$B$_{g.s.}$	5.18 ± 0.04	360 ± 50	13.6 ± 4.1
1		6.54 ± 0.03	300 ± 50	4.2 ± 1.3
2	Democratic	5.30 ± 0.02	$\leqslant 200$	1.2 ± 0.4
2		6.57 ± 0.03	300 ± 50	1.3 ± 0.4
3	$\alpha + ^6$Be$_{g.s.}$	6.5	–	<1

For events without the ^{8}Be$_{g.s.}$ correlation, two further groups of events were obtained based on gates set on the ^{6}Be$_{g.s.}$ and ^{9}B$_{2nd}$ peaks in Figs. 4(c) and 4(d). The $E^*(^{10}\mathrm{C})$ distributions for these events are displayed in Figs. 3(d) and 3(e). These spectra show no statistically significant peaks. The levels associated with the ~5.2 MeV peaks in the first two groups are subthreshold for $\alpha + ^6$Be$_{g.s.}$ and $p + ^9$B$_{2nd}$ decay. One cannot rule out a small contribution to the ~6.5 MeV peak from $\alpha + ^6$Be$_{g.s.}$ decay [see Fig. 3(d)] and Table I provides a limit to this cross section.

For the second class of events where neither of the two protons are strongly correlated with ^{8}Be$_{g.s.}$, one could consider the possibility of a sequential two-proton decay through the very-wide first excited state ($E^* = 1.5$ MeV, $\Gamma = 1.2$ MeV) of ^{9}B (see Fig. 1). For the 5.30 MeV state of ^{10}C, such a decay is only possible through the low-energy tail of this wide state. Now, the average energies of the emitted protons in the $2p + 2\alpha$ center-of-mass frame for the 5.30 and 6.57 MeV states are 0.6 and 1.1 MeV, respectively. As these energies are of the same order as, or smaller than, the width of the intermediate state, then one cannot really consider such a decay as sequential, where the two proton emissions are separated in time and are independent, except for conservation laws. This situation is similar to the decay of the ground and excited states of ^{6}Be to the $2p + \alpha$ channel where the possible ^{5}Li$_{g.s.}$ intermediate has a width of $\Gamma = 1.5$ MeV. Bochkarev *et al.* [5,6] call these decays democratic and for the first excited state of ^{6}Be (2^+), they deduce that the correlations between the decay fragments are related to the $2p + \alpha$ structure of parent state. On the other hand, for the ground state (0^+) this is less clear. Therefore it is of interest to

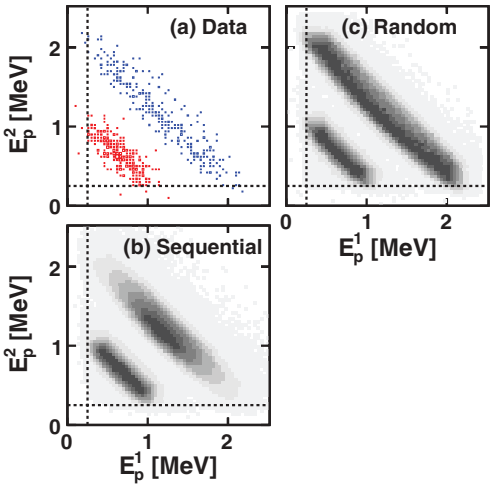

FIG. 5. (Color online) Distributions of the two proton energies in the ^{10}C center-of-mass frame for the two excited states at $E^* = 5.30$ and 6.57 MeV for events from group two: (a) Experimental distribution. Simulated distributions are shown for (b) sequential and (c) random decay. The dashed lines indicate approximate thresholds associated with the ^{9}B$_{g.s.}$ gate.

more closely examine the correlations in the second group of events.

As the ^{8}Be$_{g.s.}$ fragment constitutes most of the mass of the decaying system, it basically defines the center of mass. Therefore the kinetic energy released in the decay is approximately subdivided between the two protons. Thus in two-dimensional plots of the two proton energies (E_p^1 versus E_p^2), the events from one state should lie on a diagonal where the sum of the two energies is approximately constant. Figure 5 shows the two expected diagonal bands obtained after gating on the two observed peaks. The yield along both of the diagonals is approximately uniform. The diagonals do not extend all the way to the E_p^1 or E_p^2 axes, because such a low-energy proton would be identified as part of a ^{9}B$_{g.s.}$ correlation and the event would then belong in the first group. The dashed lines parallel to the E_p^1 and E_p^2 axes indicate roughly the threshold for this misclassification. It appears that for both states, a fraction of the these events have been misclassified as belonging to the first class. This has not been accounted for in the cross sections of Table I.

The gate on the 5.30 MeV state is quite clean, but the 6.57 MeV peak sits on a significant background. We estimate that roughly 35% of the events in the 6.57 MeV gate are background. To estimate the effect of this background, we created a gate on the adjacent higher-energy region of the $E^*(^{10}\mathrm{C})$ spectrum. The associated diagonal in the E_p^1-E_p^2 plot was also approximately uniformly distributed. Thus it does not seem that the presence of the background is producing gross distortions.

Two types of Monte Carlo simulations were performed as baselines to gauge the magnitude of the correlations between the protons. The first simulation [Fig. 5(b)] treated the decay as if it were a sequential two-proton emission passing through the wide $E^* = 1.5$ MeV first excited state of ^{9}B. The emission of the two protons was assumed independent and isotropic. The latter is of little consequence for the E_p^1-E_p^2 plots as these are sensitive to the energy partition and not to angular correlations. The energy distribution of the first emitted proton was taken as

$$P(E_p) = T(E_p)BW(E^* - S_p - E_p, E_1, \Gamma_1), \qquad (1)$$

where $BW(E, E_1, \Gamma_1)$ is a Breit-Wigner distribution for this wide state ($E_1 = 1.5$ MeV, $\Gamma_1 = 1.2$ MeV). The transmission coefficient was taken as a Fermi function,

$$T(E_p) = 1/\{1 + \exp[-(E_p - E_B)/d_B]\} \qquad (2)$$

with Coulomb barrier $E_B = 1$ MeV and $d_B = 0.25$ MeV estimated from an optical-model analysis of $p + ^{10}$B elastic-scattering data [18]. The barrier was taken for $\ell = 0$, but for larger ℓ-waves, the predicted E_p^1-E_p^2 correlations are even less like the experimental data. In the second simulation [Fig. 5(c)], the phase space of the two protons and the ^{8}Be$_{g.s.}$ fragment was sampled randomly within the constraints of energy and momentum conservation [19].

For the 5.30 MeV state (lower diagonal), the simulated distributions are similar and both are consistent with the experimental distribution. However for the 6.57 MeV state (upper diagonal), only the random simulation which predicts a uniform distribution along the diagonal is consistent with the experimental data. In the sequential simulation, decay to the centroid of the intermediate state removes roughly half the available kinetic energy. Thus the sequential simulation favors decays where the two protons have similar energies. As this is not observed in the experimental data, it suggests that this intermediate state does not play a large role in the decay and one should consider a more direct two-proton emission.

A complementary quantity of interest is the relative emission angle $\theta_{\mathrm{rel}}^{pp}$ between the two protons in the $2\alpha + 2p$ center of mass. The distributions of this quantity for the two states are plotted as the histograms in Fig. 6. The solid and dash curves give the predictions of the random and sequential simulation, respectively. Neither of these simulations consider the effect of angular momentum on the emission directions of the particle. This is known to induced angular correlations between successively emitted particles, however the θ_{rel}^{pp}

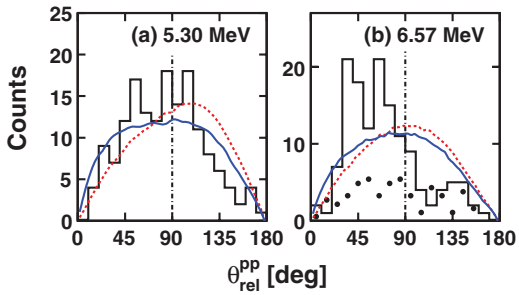

FIG. 6. (Color online) Distributions of relative angle between the two protons for events from group two. Panels (a) and (b) give the distributions gated on the 5.30 MeV and 6.57 MeV peaks, respectively. The histograms are experimental data. The data points in (b) are an estimate of the background contribution. The solid and dashed curves are predictions from the random and sequential simulations, respectively.

distributions will remain symmetric about $\theta_{rel}^{pp} = 90^{\circ}$ [20]. The small deviations from symmetry of the simulated distributions in Fig. 6 are a result of detector bias and recoil effects. For the 6.57 MeV state [Fig. 6(b)], the experimental data shows a strong asymmetry about $\theta_{rel}^{pp} = 90^{\circ}$ which is inconsistent with both simulations. Because the experimental distribution is asymmetric, angular momentum cannot be invoked to explain the failure of the simulations to reproduce the data. Also the data points in Fig. 6(b) indicate the distribution from the background gate. This background is clearly not responsible the observed asymmetry. Therefore in the decay of the 6.57 MeV state, the emission of the two protons show correlations beyond those resulting from conservation laws. Both protons are emitted preferentially on the same side of the decaying ^{10}C fragment. The nature of the correlations for the 5.30 MeV state is less clear; both simulations have a similar level of agreement with the data.

In conclusion, the particle decay of ^{10}C excited states have been studied using an $E/A = 10.7$ MeV ^{10}C beam incident on a ^{9}Be target. For $2p + 2\alpha$ exit channel, excited states were observed which decay by two-proton emission to the unstable ground state of ^{8}Be. These include states at 5.18 and 6.54 MeV where the two-proton decay is sequential in nature, passing through the long-lived ^{9}B ground state. There are also states at 5.30 and 6.57 MeV for which the two-proton emission is democratic, i.e., there exists no long-lived intermediate. The higher-energy peaks for both decay modes are consistent in energy and width and may correspond to two decay branches of a single state. However, the two lower energy states are probably separate levels. In the democratic decay of the 6.57 MeV state, the two protons are preferably emitted on the same side of the decaying ^{10}C fragment.

This work was supported by the U.S. Department of Energy, Division of Nuclear Physics under grants DE-FG02-87ER-40316 and DE-FG02-93ER40773.

[1] D. R. Tilley *et al*., Nucl. Phys. **A745**, 155 (2004).
[2] Y. Kanada-En'yo and H. Horiouchi, Prog. Theor. Phys. Suppl. **142**, 205 (2001).
[3] M. Freer *et al*., Phys. Rev. Lett. **96**, 042501 (2006).
[4] R. A. Kryger *et al*., Phys. Rev. Lett. **74**, 860 (1995).
[5] O. V. Bochkarev *et al*., Nucl. Phys. **A505**, 215 (1989).
[6] O. V. Bochkarev *et al*., Sov. J. Nucl. Phys. **55**, 955 (1992).
[7] R. E. Tribble, R. H. Burch, and C. A. Gagliardi, Nucl. Instrum. Methods Phys. Res. A **285**, 411 (1989).
[8] M. S. Wallace *et al*., submitted to Nucl. Instrum. Methods Phys. Res. A.
[9] G. L. Engel *et al*., Nucl. Instrum. Methods Phys. Res. A **573**, 418 (2007).
[10] J. F. Ziegler, J. P. Biersack, and U. Littmark, *The Stopping and Range of Ions in Solids* (Pergamon Press, New York, 1985); the code SRIM can be found at www.srim.org.
[11] A. A. M. Mustafa *et al*., Phys. Med. Biol. **26**, 461 (1981).
[12] M. Mangelson, F. Ajzenberg-Selove, M. Reed, and C. C. Lu, Nucl. Phys. **88**, 137 (1966).
[13] W. Benenson, G. M. Crawley, J. D. Dreisbach, and W. P. Johnson, Nucl. Phys. **A97**, 510 (1967).
[14] B. Höistad *et al*., Phys. Rev. Lett. **43**, 487 (1979).
[15] G. J. Lolos *et al*., Phys. Rev. C **25**, 1082 (1982).
[16] L. Wang *et al*., Phys. Rev. C **47**, 2123 (1993).
[17] M. J. Schneider *et al*., Phys. Rev. C **12**, 335 (1975).
[18] B. Zwieglinski, J. Piotrowski, A. Saganek, and I. Sledzinska, Nucl. Phys. **A209**, 348 (1973).
[19] J. Randrup, Comput. Phys. Commun. **59**, 439 (1990).
[20] L. Biedenharn and M. Rose, Rev. Mod. Phys. **25**, 729 (1953).